Future Journal of Pharmaceutical Sciences

RESEARCH Open Access

In vitro kinetic release study of ketoprofen enantiomers from alginate metal complexes

Ghaidaa Alkhayer[1,2*], Hussein Khudr[2] and Yahia Koudsi[1]

Abstract

Background: To explore the release behavior of ketoprofen enantiomers from alginate-metal-complexes. Five mathematical models of drug release kinetics were investigated.

Results: Beads of alginate-metal complexes, loaded with racemic ketoprofen, were prepared by the ionotropic method. Divalent (Ca, Ba, Zn) and trivalent (Fe, Al) metals were used in the preparation of single-metal and mixed-metal alginate complexes. In vitro release experiments were carried out in an aqueous phosphate buffer medium at pH = 7.4. The concentrations of ketoprofen released enantiomers were determined using chiral HPLC technique. The obtained data were used to simulate the release kinetic of ketoprofen enantiomers using various mathematical models. The Korsmeyer-Peppas model was the best fit for Ca, Al, and Fe beads. Moreover, alginate-iron beads tend to release the drug faster than all other cases. In contrast, the drug release for alginate-barium complex was the slowest. The presence of barium in alginate mixed-metal complexes reduced ketoprofen release in the case of Fe and Zn, while it increased the release in the case of Al complex.

Conclusion: In all the studied cases, ketoprofen showed very slow release for both enantiomers over a period exceeded 5 h (10 days in some cases). The release rate modification is possible using different multivalent metals, and it is also feasible by using two different metals for congealing either consecutively or simultaneously.

Keywords: Alginate, Ketoprofen, Kinetics, Chiral HPLC

Background

Designing sustained drug delivery systems is a precedence challenge for researchers who are working hard to minimize the side effects of drugs and maximize the benefits at the same time. The properties, advantages (including lowering cost), disadvantages, and applications of such modified and controlled release systems were discussed and criticized often recently [1, 2]. However, numerous reviews also discussed and described drug release kinetic models and mechanisms [3–6]. In this context, however, ketoprofen, an important non-steroidal anti-inflammatory chiral drug [7], known to have short half-life time, has been studied in different formulae and matrices for sustained release, controlled release, and dissolution enhancement [8–18], tablets [19–21], patches [22], fibers [23], and beads [24]. On the contrary, the release kinetics of ketoprofen enantiomers from chiral matrices was rarely studied [25].

Alginate (Fig. 1), a chiral polysaccharide, forms cross-linked hydrogels when complexed with suitable multivalent metal ions [26–28]. Subsequently, the ionotropic gelling technique evolves continuously and alginate becomes responsible for many drug-modified delivery systems as the resulted gel networks can confine small molecule drugs [29–34].

In our previous work [35], the prepared alginate metal complexes' beads were characterized in terms of size,

* Correspondence: Ghaidaa.S.AlKhayer@gmail.com
[1]Department of Chemistry, Faculty of Sciences, Damascus University, Damascus, Syria
[2]Research Institute for Pharmaceutical and Chemical Industries, Scientific Studies and Research Centre, Damascus, Syria

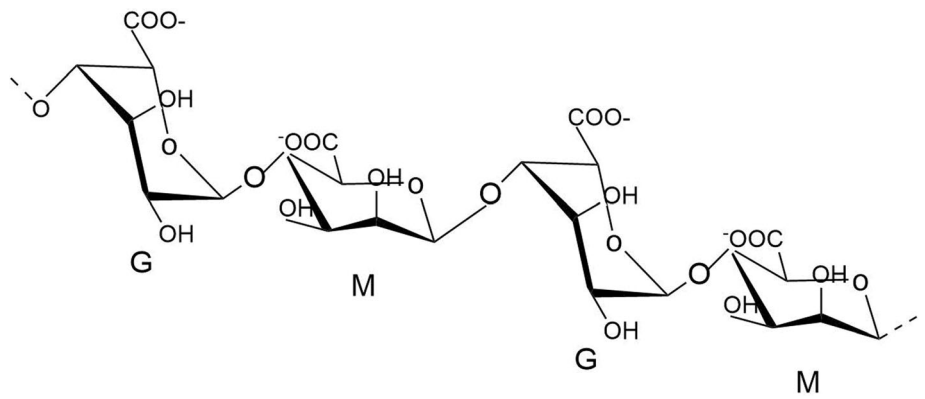

Fig. 1 Structure of sodium alginate: M, mannuronic acid; G, guluronic acid

metal content, drug content, and drug loading efficiency. Moreover, IR spectra were used to explore possible chiral interactions between the chiral drug and the chiral matrix. Therefore, chiral HPLC was exploited to monitor the probable enantioselective release of the drug from the chiral matrix. The HPLC results showed notable release selectivity in favor of S-enantiomer in the case of alginate-calcium complex.

This work aims to explore the effect of complexing multivalent metal ion on the release kinetics of ketoprofen enantiomers from alginate-metal beads. Thus, common mathematical models of drug release were investigated. Subsequently, a better understanding could result in using these complexes in sustained-release matrixes, or may be in enantioselective release matrices.

Methods and materials

Alginic acid sodium salt was purchased from brown algae BioReagent, suitable for immobilization of microorganisms from Sigma-Aldrich. (S)-Ketoprofen was from Sigma-Aldrich; assay 99%, calcium chloride, iron chloride, aluminum chloride, barium chloride dehydrate, and zinc chloride were obtained from Merck. Racemic ketoprofen (KTP) was from Infinity Laboratories Private Limited (Infinity, India) 99.6%. All other chemicals and reagents used were of analytical grade or HPLC grade.

Instrumentations and methods

HPLC chiral analysis conditions were HPLC-LC-20AD Shimadzu-Japan, equipped with photodiode array detector, manual Rheodyne injector (model 7125, 20 µl loop), and Lab solution software. The used mobile phase contained hexane, isopropanol, and TFA with 90:10: 0.1 v/v% ratios respectively. The flow rate was 1 ml/min. The used chiral column was Kromasil®-5-amy coat (250 × 4.6 mm i.d) 5 µm. The HPLC analytical method was described in details in our previous work [33].

Beads were prepared using ionotropic congealing method in which, racemic KTP was dissolved in sodium alginate aqueous solution PBS, pH = 7.4 to obtain 2% (weight/volume) alginate solution in a ratio of KTP to sodium alginate 1 to 3.75 (w/w). The obtained solution was then congealed in a bath contained a metal chloride (3% w/v) at room temperature. The formed beads were stirred continuously in the solution for 24 h, separated and washed with PBS and distilled water for 1 min; then, the beads were dried at 40 °C for 48 h, and the described details were in [33]. However, dried beads were released in phosphate buffer solution (PBS) of pH = 7.4 to simulate that of gastric medium (6.8–7.4). Aliquots, at different time intervals, were taken, extracted, and analyzed using chiral HPLC to follow the KTP enantiomers concentrations in the release medium.

Optical microscope zoom 2000 from Leica microsystem use for imaging the surface of samples, Germany. Photos of dried beads were taken with × 40 magnification.

Drug release kinetics modeling

Zero-order, first-order, Higuchi, Hixon-Crowell and Korsmeyer-Peppas models were abundantly used in the literature to simulate ketoprofen release kinetics from various matrices [9–13, 15, 16, 20, 36]. These models described in Tables 1 and 2, and they will be exploited in this work to study the ketoprofen release from the prepared alginate metal complexes beads.

Results

Beads' characteristics

A summary of beads characteristics, congealing conditions, bead size, and shape are shown in Table 3.

In vitro ketoprofen release study

Release study of KTP in PBS (pH 7.4)

Concentrations of released KTP enantiomers were determined quantitatively (µg/ml) in the withdrawn aliquots using chiral HPLC. The intent of using this analysis

Table 1 description of some mathematical models used to determine drug release from drug delivery systems

Zero-order	$Q_0 - Q_t = K_0 t$	Q_t is the drug released amount at time t; Q_0 is the initial concentration of drug at time. K_0 is the release constant of zero-order kinetic
First-Order	$\log Q_r = \log Q_0 - K_1 t/2.303$	Q_r is the drug remaining amount at time t, K_1 is the release constant of first-order kinetic.
Higuchi	$Q = K_H * t^{1/2}$	K_H is the release constant of Higuchi Kinetic
Hixson-Crowell	$Q_0^{1/3} - R_t^{1/3} = K_{HC} t$	R_t is the drug remaining amount at time t; K_{HC} is the release constant of Hixson-Crowell Kinetic.
Korsmeyer-Peppas	$Q_t/Q_\infty = K_{kp} * t^n$	Q_t/Q_∞ is a drug released fraction at time t, n is the diffusional exponent or drug release exponent, and K_{kp} is the release constant of Korsmeyer-Peppas Kinetic

In Korsmeyer-Peppas equation, n characterizes different release models for different shaped matrices as summarized in Table 2

technique is observing each KTP enantiomers as enantioselective release is probable. This probability come from chiral interactions established between chiral drug and used chiral matrices [20, 25, 35].

However, chiral KTP analysis results are expressed in terms of enantiomeric excess ee% as showed in Table 4 for the first 2 h of the release experiment. The ee% is given by the expression ee% = $\left| (R - S)/(R + S) \right|$.

Before modeling the KTP release from the prepared beads, we defined release rate R_L to be used in comparing between release behaviors of various beads. R_L could be described as the concentration alteration C_t over a specified time T, i.e., $R_L = C_t/T$ (μg ml^{-1} h^{-1}). The specified time T was chosen to be equals to the half-life time of KTP, i.e., 2 h. Bearing in mind that the total volume of release solution is conserved as the volume loss because of withdrawn aliquots was compensated by equal volume addition of PBS solution.

The KTP released quantity percentages, for all beads kinds, were plotted against time as depicted in Figs. 2, 3, 4, and 5. Typical HPLC chromatograms for different alginate beads are also presented in Figs. 6 and 7.

Table 2 Summary of different release characteristics depending on release exponent n of Korsmeyer-Peppas [37]

Release mechanism model	Geometry	Release exponent (n)
Fickian diffusion	Planar (thin films) Cylinders Spheres	0.50 0.45 0.43
Anomalous transport	Planar (thin films) Cylinders Spheres	$0.50 < n < 1.0$ $0.45 < n < 0.89$ $0.43 < n < 0.85$
Case I transport	Planar (thin films) Cylinders Spheres	1.0 0.89 0.85
Super Case II transport Planar	Planar (thin films) Cylinders Spheres	$n < 1.0$ $n < 0.89$ $n < 0.85$

Modeling KTP release kinetics

The required data to model the release kinetics of KTP from the prepared single-metal alginate complexes were obtained and used to find the best-fit models. Table 6 summarizes the resulted correlation coefficient R^2 and the release kinetic constants corresponding to each studied model.

Discussion

The shape and size of beads varied depending on complexing ion metal; the divalent ion beads are smaller in size (5–7-mm diameter for wet and 2–3 mm for dry beads) than trivalent ion beads (7–10-mm diameter for wet, 2–3.5 mm for dry beads). The beads' shape was not a regular sphere; it is tear-like for Ca and Ba beads, full of sharp uplifting for Zn and Al beads, and middle-collapsed for Fe beads. All beads also have their characteristic convolutions and wrinkles. It may be probable that these differences in shape and morphology have an impact on the release behavior of the studied drug. Table 3 summarizes the characteristics of the formed beads.

Effect of complexing ion metal on the KTP enantiomers release behavior

In our previous work [35], we gave proof of chiral interactions between ketoprofen and alginate. These interactions, believed to lead to enantioselective release under certain conditions, are mainly due to hydrogen bindings between the carboxylic group of the drug and carboxylic and hydroxyl groups of alginate; similar interactions were proved between tiaprofenic acid and alginate [38]. During, the release experiment, water molecules will participate in hydrogen bonding while penetrating the beads networks. Subsequently, the prescribed chiral interactions will be less strong resulting in decreased ee% values. This logic applies to all the studied cases in Table 4 and there is no contradiction between the Fe case and the other cases. However, the tabulated ee% values can be understood as the following: ee% values marked with asterisk* are smaller or close to 1%, and they more likely indicate racemic release and not necessarily indicate an

Table 3 Shape, size, and congealing conditions of the prepared beads used in this study

Single metal complexes					
	ABaK	ACaK	AZnK	AAlK	AFeK
Dry beads (x 40)		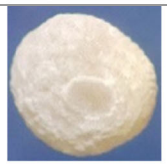		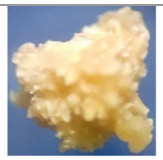	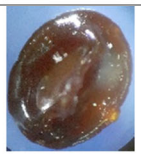
Bead size (mm)/ wet			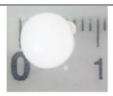	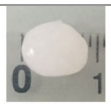	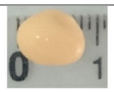
Congealing conditions	3% $BaCl_2$ 24h	3% $CaCl_2$ 24h	3% $ZnCl_2$ 24h	3% $AlCl_3$ 24h	3% $FeCl_3$ 24h
Mixed metal complexes					
	ABaCaK	ABaZnK	ABaAlK	ABaFeK	
Dry beads (x 40)		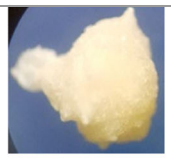	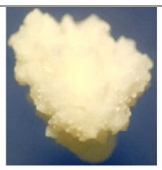	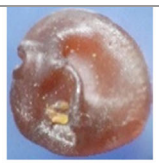	
Bead size (mm)/ wet				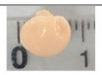	
Congealing conditions	3% $BaCl_2$ 3h + 3% $CaCl_2$ 21h	3% $BaCl_2$ 3h + 3% $ZnCl_2$ 21h	3% $BaCl_2$ 3h + 3% $AlCl_3$ 21h	3% $BaCl_2$ 3h + 3% $FeCl_3$ 21h	
	A_1K	A_2K	A_3K		
Dry beads (x 40)		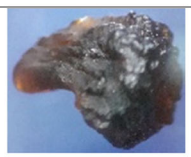			
Bead size (mm)/ wet					
Congealing conditions	3% $CaCl_2$ 24h + 3% $FeCl_3$ 24h	3% $CaCl_2$ 3h + 3% $FeCl_3$ 21h	3% $FeCl_3$ 3h + 3% $CaCl_2$ 21h		

*Metal chloride concentration (%), time of congealing (h)

Table 4 Obtained ee% results for 120 min in the release medium

Time (min)		10	20	30	40	50	60	75	90	120
ee%	ACaK	35.2 (S)	27.6 (S)	18.4 (S)	10.4 (S)	0.3 (S)	0.1 (R)*	0.2 (R)*	0.3 (R)*	0.8 (S)*
	AZnK	13.7 (R)	7.2 (R)	7.0 (R)	6.7 (R)	7.5 (R)	7.1 (R)	6.4 (R)	7.0 (R)	6.9 (R)
	AAlK	10.3 (R)	4.9 (R)	5.6 (R)	8.0 (R)	9.2 (R)	3.2 (R)	2.5 (R)	6.9 (R)	1.2 (S)*
	AFeK	0.4 (R)*	0.7 (S)	1.2 (S)	1.5 (S)	1.5 (S)	1.6 (S)	1.6 (S)	1.7 (S)	1.6(S)

*: refers to inhomogenious chiral interactions

inversion of the release enantioselectivity. In the case of ACaK beads, the release began in favor of the S-enantiomer of KTP with ee% = 35.2, the highest value in the table. This value decreased gradually with time increase to reach the value of 0.3 after 50 min. After that, the R-enantiomer released favorably with relatively the smallest ee% values in the table. In contrast, for AZnK and AAlK beads, the R-enantiomer released selectively with comparable starting ee% values of 13.7 and 10.3 respectively. Additionally, in the case of AFeK beads, the starting ee% values (marked with asterisk*) can be viewed as a result of inhomogeneous chiral interactions which became homogeneous lately indicating selective release of S-enantiomer. However, ee% values, after 30 min, fluctuate between 1.5 and 1.7 showing a more stable trend rather than an increasing one. Nonetheless, understanding the ee% results, hence the related enantioselective release process needs more understanding of many factors that can affect the process such as drug load and drug distribution within the bead, bead shape, and porosity [39].

The results of ABaK beads are not shown because of the very weak concentrations of the released enantiomers. Nonetheless, the ACaK beads showed the most dramatic changes in ee% results. Thus, curves shown in this study represent the sum of both released enantiomers.

As previously described [40, 41], metals bind with different strength to alginate forming alginate-metal complexes with "egg-box" structures. The related strength follows the order Sr^{2+}>Pb^{2+}> Ca^{2+}>Cd^{2+}>Mg^{2+}>Fe^{2+}>-Fe^{3+}>Co^{2+}>Al^{3+}. Hence, the strongest the complex the slowest dissociation, and subsequently the faster drug release from the complex. This explain the obtained results shown in Table 5, where R_L values for single metal alginate beads follow the order AFeK>AAlK>AZnK>ACaK>ABaK. Similar results were also obtained for the drug quantity released after 30 min. This quantity, Q_{30}, was considered the onset release quantity (μg),

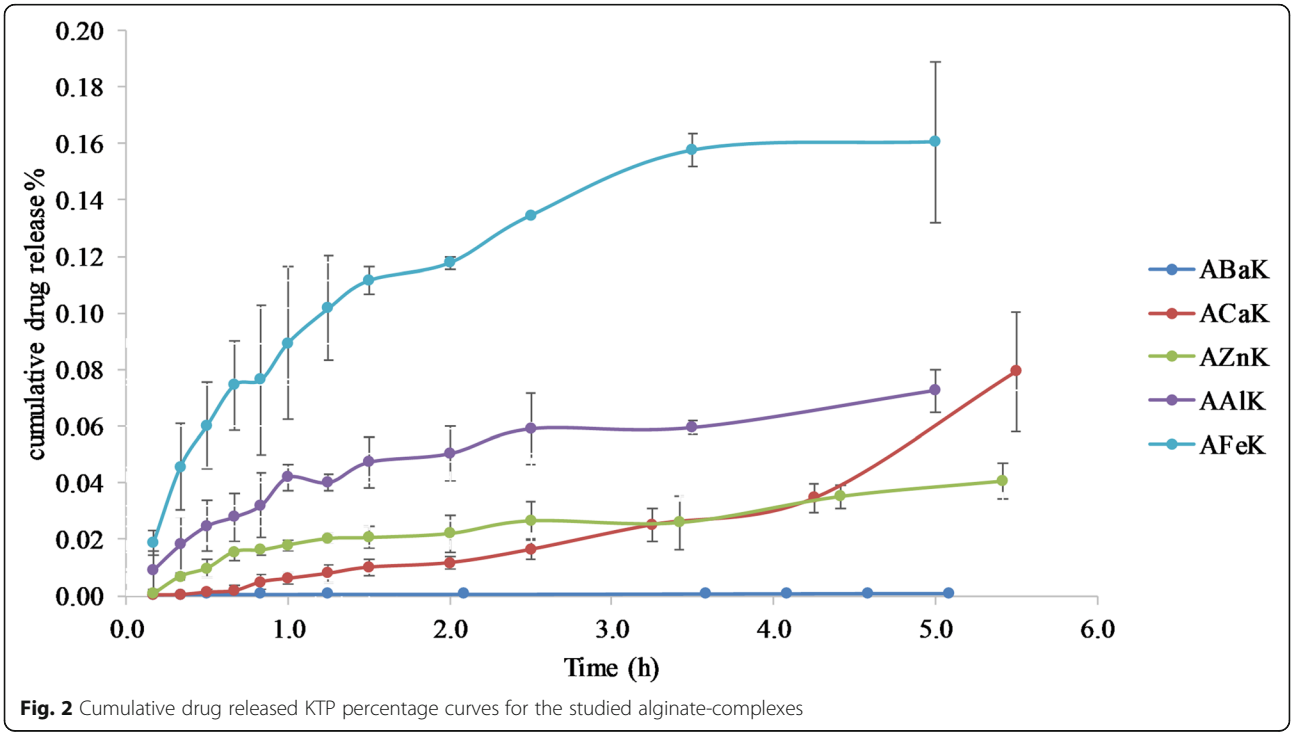

Fig. 2 Cumulative drug released KTP percentage curves for the studied alginate-complexes

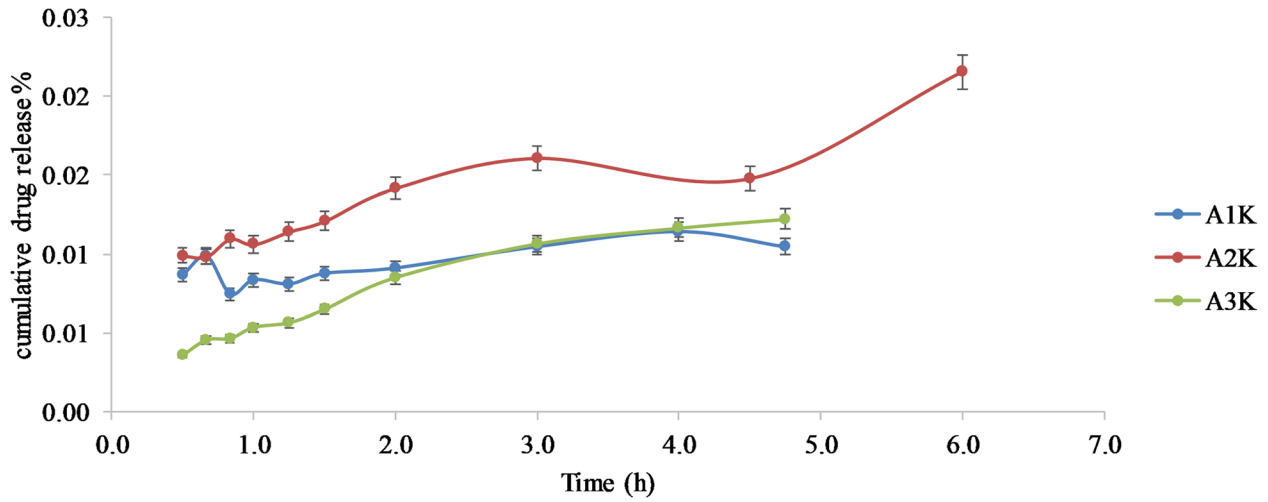

Fig. 3 Cumulative released KTP percentage curves for simultaneously (A_1K) and consecutively congealed beads (A_2K, A_3K) with Ca and Fe

according to which the studied complexes followed the same order as above AFeK>AAlK>AZnK>ACaK>ABaK. Generally, the onset release concentrations and the release rates were higher in the case of trivalent metal complexes compared to those of divalent metal complexes. Thus, this could be because the studied divalent metals form stronger complexes with alginate compared to those of the studied trivalent metals.

Effect of congealing sequence with two ion metals on the KTP enantiomers release behavior

In the case of co-congealing with Ca and Fe, the simultaneous congealed beads A_1K have the slowest rate compared to those of consecutive congealed A_2K (Ca then Fe) and A_3K (Fe then Ca). The relevant release curves are depicted in Fig. 3. An interesting difference between A_1K and A_3K behaviors was noticed; over

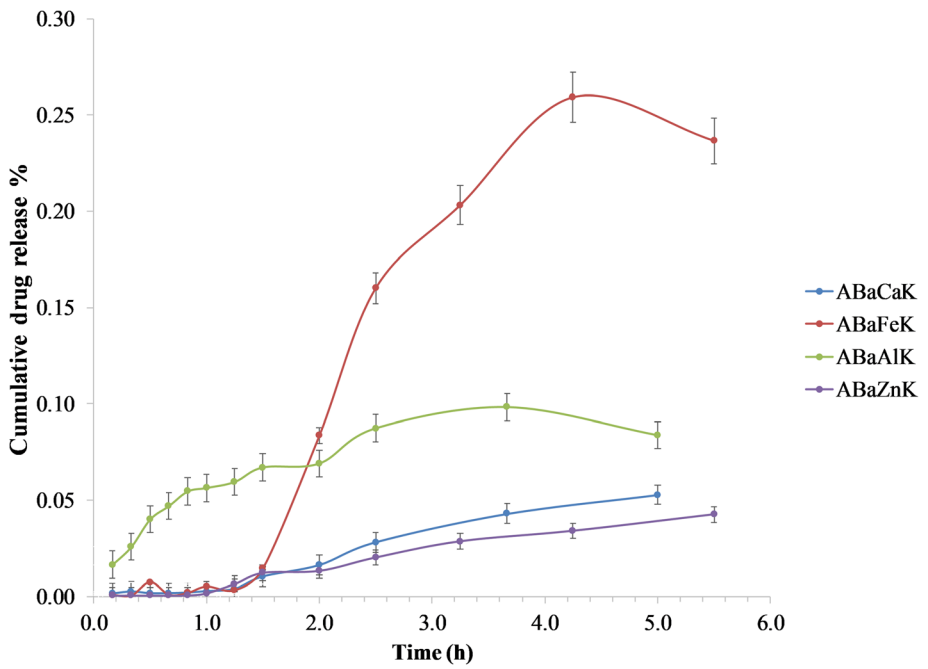

Fig. 4 Cumulative released KTP percentage curves for consecutive congealed beads (ABaCaK, ABaFeK, ABaAlK, ABaZnK), 5.5-h experiment

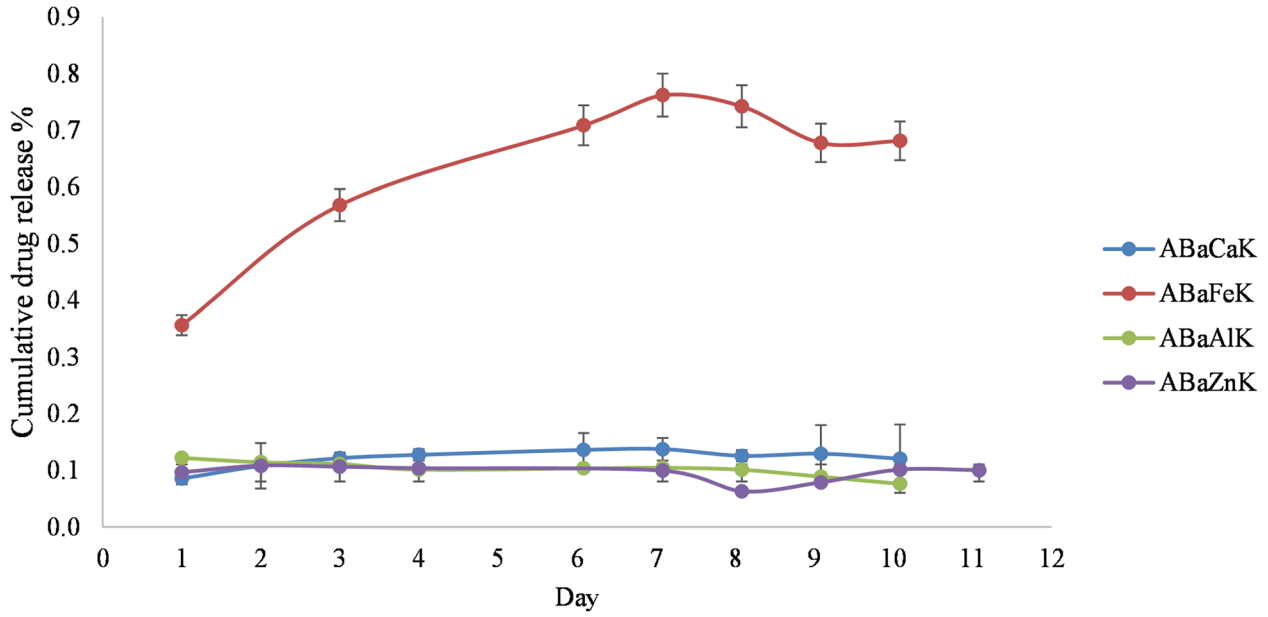

Fig. 5 Cumulative released KTP percentage curves for consecutive congealed beads (ABaCaK, ABaFeK, ABaAlK, ABaZnK), 10-day experiment

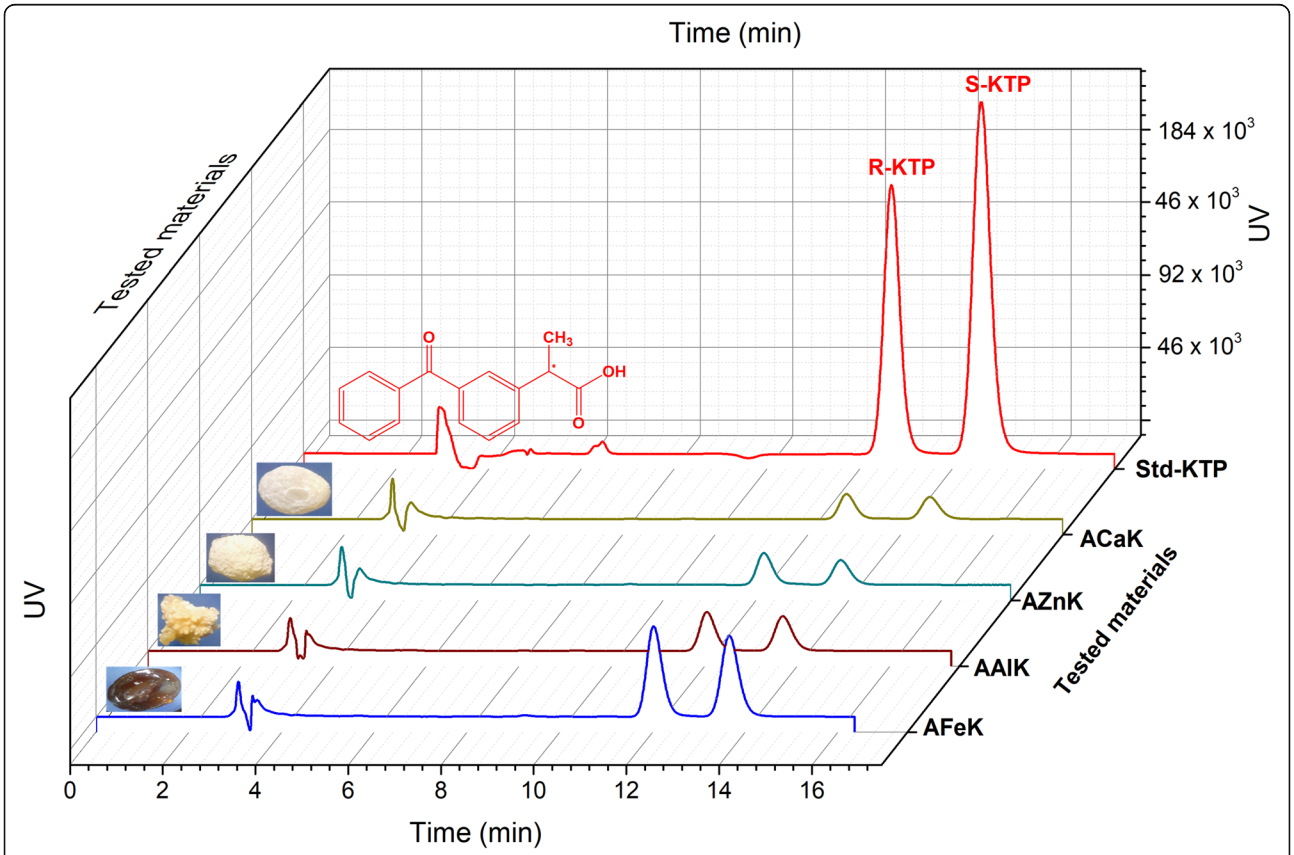

Fig. 6 HPLC chromatograms for mixed beads complexed with Ba (ABaCaK, ABaZnK, ABaAlK, ABaFeK) and mixed beads with Ca and Fe; simultaneous (A_1K) and consecutive (A_2K, A_3K) congealed method

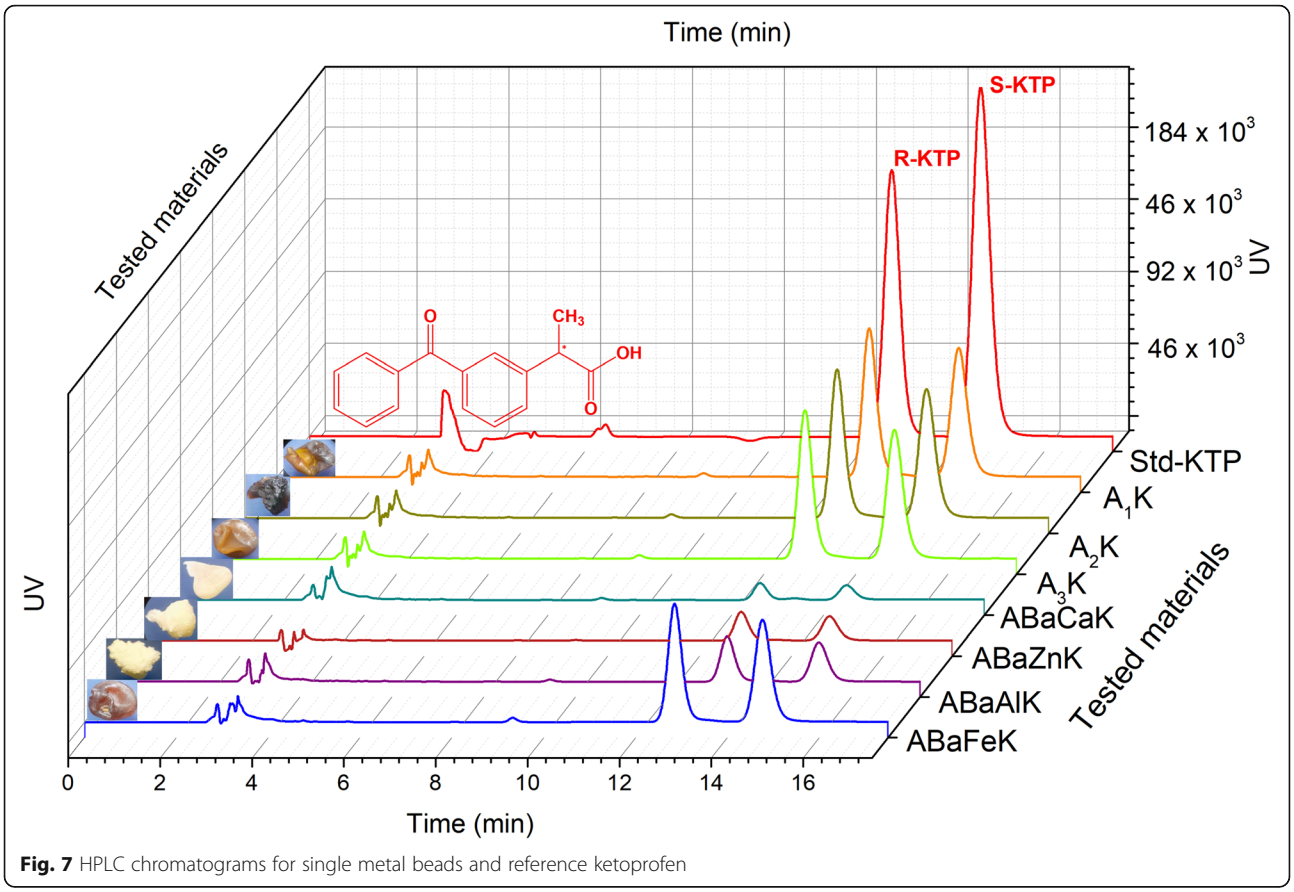

Fig. 7 HPLC chromatograms for single metal beads and reference ketoprofen

the first 50 min (approx) A_3K showed slower release than A_1K but after that period the release rate of A_3K became the faster. Thus, this indicates an obvious effect of altering congealing sequences on the related release behaviors.

According to R_L values of the mixed metals' beads prepared with Ba and other metal as described in Table 3, beads can be ordered as ABaFeK>ABaAlK>ABaZnK>ABaCaK. However, the related curves of cumulative released drug percentage, shown in Fig. 4, indicated similar trends for ABaCaK and ABaZnK beads (Ba mixed with divalent metals) different from those of ABaFeK and ABaAlK beads (Ba mixed with trivalent metals). This again shows the different behavior of the complexes with trivalent metals from those of divalent metals. Thus, this was due to the differences in binding strengths and the resulted network structures (egg-box structures). ABaFeK and ABaAlK beads have similar R_L; the same point at 2 h as in Fig. 4, but they have different curves over the experiment time of 6 h (Fig. 4) and also for 10 days as shown in Fig. 5.

Additionally, during the experiment time for all kinds of these beads, cumulative release curves showed much less than 1% released drug. The curves also did not show flat or decreasing parts, i.e., KTP concentrations did not reach the maximum or the equilibrium state in the release medium. Thus, this indicated sustainability over the experiment time; however, a significant release drug has not been accomplished yet.

The KTP release model

Before trying to interpret the results, it is important to recall that the studied beads have different shapes and morphologies. Enantiomers release kinetics were modeled for single-metal alginate complexes. However, Table 6 contains the obtained results for each released enantiomer and the sum of released enantiomers.

Table 5 Rate and onset quantity results obtained for alginate metal complexes beads

	ACaK	AZnK	AAlK	AFeK	ABaCaK	ABaZnK	ABaAlK	ABaFeK
R_L	0.55	0.75	1.60	3.65	0.56	0.64	2.92	2.95
Q_{30}	0.51	5.31	8.18	18.80	0.54	0.31	16.92	2.62

Table 6 Results of modeling KTP release kinetics

Beads		Zero-order		First-order		Higuchi		Hixson-Crowell		Korsmeyer-Peppas	
		R^2	K_0	R^2	K_1	R^2	K_H	R^2	K_{HC}	R^2	n
ACaK	R	0.887	0.01	0.887	$-6e^{-5}$	0.799	0.04	0.955	− 0.001	0.957	1.56
	S	0.882	0.01	0.882	$-6e^{-5}$	0.793	0.04	0956	− 0.001	0.965	1.53
ACaK[a]		**0.884**	**0.01**	**0.884**	$\mathbf{-6e^{-5}}$	**0.796**	**0.04**	**0.955**	**− 0.001**	**0.961**	**1.55**
AZnK	R	0.942	0.01	0.942	$-2e^{-5}$	0.946	0.02	0.942	− 0.001	0.931	0.48
	S	0.945	0.01	0.947	$-2e^{-5}$	0.947	0.02	0.946	− 0.001	0.933	0.49
AZnK[a]		**0.945**	**0.01**	**0.945**	$\mathbf{-2e^{-5}}$	**0.928**	**0.02**	**0.944**	**− 0.001**	**0.932**	**0.49**
AAlK	R	0.888	0.01	0.888	$-4e^{-5}$	0.951	0.03	0.889	− 0.001	0.954	0.46
	S	0.887	0.01	0.887	$-4e^{-5}$	0.949	0.03	0.889	− 0.001	0.952	0.46
AAlK[a]		**0.888**	**0.01**	**0.888**	$\mathbf{-4e^{-5}}$	**0.950**	**0.03**	**0.889**	**− 0.001**	**0.953**	**0.46**
AFeK	R	0.886	0.02	0.886	$-1e^{-4}$	0.958	0.07	0.883	− 0.002	0.974	0.44
	S	0.884	0.02	0.884	$-1e^{-4}$	0.957	0.07	0.880	− 0.002	0.972	0.44
AFeK[a]		**0.882**	**0.02**	**0.882**	$\mathbf{-1e^{-4}}$	**0.956**	**0.07**	**0.881**	**− 0.002**	**0.972**	**0.44**

[a]Sum of released enantiomers

Moreover, the simulated data resemble only the release profile of a very small fraction of the loaded KTP. This fraction did not arrive at 1% even after 10 days of release time. From this point of view, the best-fit model derived from this data is tricky and may not be comparable with other models of higher released fractions.

The best-fit model for resulted data of ACaK beads, for the total released KTP, and for each enantiomer R and S, was Korsmeyer-Peppas model as it has the highest correlation coefficient values. For ACaK beads, the release showed super case-II transport indicating more than one release mechanism ($n > 0.85$, it is 1.55, 1.56 and 1.53 for ACaK, ACaK-R, and ACaK-S respectively). Thus, the observed enantioselective release did not result from different release kinetics of each enantiomer. Simulating KTP release from AZnK beads did not result in a clear one best-fit model; Zero-order, First-order, and Hixon-Crowell models are quasi-equally probable as the related R^2 values are comparable. From first glance, this is unreasonable; the obtained data cannot follow three different models. However, to explain this, it is fair to remember that models can be similar to a short-range of data. The studied cases herein represent less than 1% release. However, the release obeyed the Korsmeyer-Peppas model with an anomalous mechanism in the case of AAlK ($n = 0.46$) and AFeK ($n = 0.44$) beads, for each enantiomer and the sum of enantiomers.

It is noteworthy that a complete KTP release was achieved from alginate-calcium beads after 3 h and no enantioselective release was reported. However, the mentioned beads were prepared in different conditions. They were congealed in 0.1 M solution of $CaCl_2$ within 12 h, dried 24 h at RT and subsequent 24 h at 45 °C [42]. Comparing these conditions with our conditions indicates that increasing the concentration of calcium ions will decrease drug release. On the other hand, increasing the congealing time will also decrease drug release.

Conclusion

Alginate-metal complexes, reported in this work, caused weak KTP release concentrations, for both enantiomers, over a long period of time (10 days in several cases). The Korsmeyer-Peppas model was the most convenient fit in the case of Ca (for both enantiomers), Al, and Fe beads. More efforts are needed to find a better kinetic model that take into consideration the shape deviation from spheres, especially in the case of iron complexes. In all the studied cases, KTP enantiomers showed the highest rate for Fe beads and the smallest for Ba ones. The release rate modification is possible using different multivalent metals, and it is also feasible by using two different metals for congealing either consecutively or simultaneously. These results suggest alginate-metal complexes as a possible precursor for KTP enantiomers sustained release systems.

Abbreviations

KTP: Ketoprofen; PBS: Phosphate buffer solution; HPLC: High-performance liquid chromatography; ee%: Enantiomeric excess

Acknowledgements

Not applicable for that section.

Authors' contributions

GK and HK contributed equally in the design of the work, acquisition and interpretation of data, and manuscript preparation. GK carried out the experimental studies. HK and YK revised the final manuscript. All authors read and approved the final manuscript.

Funding

Not applicable for that section.

Availability of data and materials
Data and materials are available upon request.

Ethics approval and consent to participate
Not applicable for that section.

Consent for publication
Not applicable for that section.

Competing interests
The authors declare that they have no competing interests.

Received: 25 April 2020 Accepted: 3 December 2020
Published online: 07 January 2021

References
1. Alhalmi A, Altowairi M, Alzobaidi N, Almoiliqy M (2018) Sustained release matrix system: an overview intestinal ischemia-reperfusion (I/R) injury view project, artic. World J Pharm Pharm Sci 7:1470–1486. https://doi.org/10.20959/wjpps20186-11835
2. Sowjanya M, Debnath S, Lavanya P, Thejovathi R, Babu MN (2017) Polymers used in the designing of controlled drug delivery system. Res J Pharm Technol 10:903–912. https://doi.org/10.5958/0974-360x.2017.00168.8
3. Dash S, Murthy PN, Nath L, Chowdhury P (2010) Kinetic modeling on drug release from controlled drug delivery systems. Acta Pol Pharm Drug Res 67:217–223
4. Ford AN, Pack DW, Braatz RD (2013) Mathematical modeling of drug delivery from autocatalytically degradable PLGA microspheres--a review. J Control Release 165:29–37
5. Kharat AR (2014) Mathematical models of drug dissolution: a review, Sch. Acad J Pharm 3:2320–4206
6. Mircioiu C, Voicu V, Anuta V, Tudose A, Celia C, Paolino D, Fresta M, Sandulovici R, Mircioiu I (2019) Mathematical modeling of release kinetics from supramolecular drug delivery systems. Pharmaceutics. 11(3):140. https://doi.org/10.3390/pharmaceutics11030140
7. Somberg J (2009) Martindale: the complete drug reference, 36th edn. Pharmaceutical Press, UK
8. Najmuddin M, Hafiz RF, Nizamuddin M, Khalid MS (2009) Development and evaluation of ketoprofen mini-matrices as sustained release formulation. Int J Chem Sci 7:2122–2134
9. Kaleemullah M, Jiyauddin K, Thiban E, Rasha S, Al-Dhalli S, Budiasih S, Gamal OE, Fadli A, Eddy Y (2017) Development and evaluation of Ketoprofen sustained release matrix tablet using Hibiscus rosa-sinensis leaves mucilage. Saudi Pharm J 25:770–779. https://doi.org/10.1016/j.jsps.2016.10.006
10. Chan SY, Chung YY, Cheah XZ, Tan EYL, Quah J (2015) The characterization and dissolution performances of spray dried solid dispersion of ketoprofen in hydrophilic carriers, Asian J. Pharm Sci 10:372–385. https://doi.org/10.1016/j.ajps.2015.04.003
11. Nagori S, Asija R, Gupta A, Garg A (2018) Formulation and evaluation of sustained release matrix tablets of ketoprofen using natural gums. Res J Pharm Technol 7:274–293. https://doi.org/10.20959/wjpps20184-11071
12. Vueba ML, Batista De Carvalho LAE, Veiga F, Sousa JJ, Pina ME (2004) Influence of cellulose ether polymers on ketoprofen release from hydrophilic matrix tablets. Eur J Pharm Biopharm 58:51–59. https://doi.org/10.1016/j.ejpb.2004.03.006
13. Alper Öztürk A, Çinar Nİ, Yenilmez E (2019) Development of nano-sized ketoprofen lysine incorporated Eudragit® S100 nanomedicine by double emulsion solvent evaporation and in vitro characterization. J Pharm Pharmacogn Res 7:47–58
14. Rashid SA, Khan GM, Haider H, Khan BA (2017) Fabrication of ketoprofen controlled-release tablets using biopolymeric hydrophilic matrices: in-vitro studies. Proc Pakistan Acad Sci Part B 54:89–102
15. Mantas A, Labbe V, Loryan I, Mihranyan A (2019) Amorphisation of free acid ibuprofen and other profens in mixtures with nanocellulose: dry powder formulation strategy for enhanced solubility. Pharmaceutics. 11(2):68. https://doi.org/10.3390/pharmaceutics11020068
16. Mita SR, Husni P, Setiyowati D (2018) In vitro permeation study of ketoprofen patch with combination of ethylcellulose and polyvynil pyrrolidone as matrix polymers. J Young Pharm 10:101–s105. https://doi.org/10.5530/jyp.2018.2s.20
17. Abdallah MH, Sammour OA, El-Ghamry HA, El-Nahas HM, Barakat W (2012) Development and characterization of controlled release ketoprofen microspheres. J Appl Pharm Sci 2:60–67. https://doi.org/10.7324/JAPS.2012.2310
18. Cheng B, Li D, Huo Q, Zhao Q, Lan Q, Cui M, Pan W, Yang X (2018) Two kinds of ketoprofen enteric gel beads (CA and CS-SA) using biopolymer alginate, Asian J. Pharm Sci 13:120–130. https://doi.org/10.1016/j.ajps.2017.10.003
19. Hafeez A, Razvi N, Talib N, Ghayas S, Anjum F, Bushra R (2019) Formulation optimization, in vitro characterization and stability studies of sustain release tablets of Ketoprofen. Pak J Pharm Sci 32:1245–1251
20. Valliappan K, Kannan K, Sivakumar T, Manavalan R (2006) Enantiospecific pharmacokinetic studies on ketoprofen in tablet formulation using indirect chiral HPLC analysis. J Appl Biomed 4:153–161. https://doi.org/10.32725/jab.2006.017
21. Jan SU, Khan GM, Khan KA, Rehman A, Khan H (2011) In-vitro release pattern of ketoprofen using ethyl cellulose ether derivatives. J Appl Pharmacol 3:24–33. https://doi.org/10.21065/19204159.3.24
22. Gaware S, Bala P, Dhobale S, Joshi A, Wagh N, Pal K, Kale SN (2016) Studies on control of erratic release of ketoprofen from commercial patches for sustained pain-relief using silica microparticles. Nano Hybrids Compos 12:88–97. https://doi.org/10.4028/www.scientific.net/nhc.12.88
23. Kenawy ER, Abdel-Hay FI, El-Newehy MH, Wnek GE (2007) Controlled release of ketoprofen from electrospun poly(vinyl alcohol) nanofibers. Mater Sci Eng A 459:390–396. https://doi.org/10.1016/j.msea.2007.01.039
24. Freitas ED, Lima BM, Rosa PCP, Silva MGC, Vieira MGA (2019) Evaluation of proanthocyanidin-crosslinked sericin/alginate blend for ketoprofen extended release. Adv Powder Technol 30:1531–1543. https://doi.org/10.1016/j.apt.2019.04.031
25. Solinís MA, De La Cruz Y, Hernández RM, Gascón AR, Calvo B, Pedraz JL (2002) Release of ketoprofen enantiomers from HPMC K100M matrices - diffusion studies. Int J Pharm 239:61–68. https://doi.org/10.1016/S0378-5173(02)00047-9
26. Patil JS, Kamalapur MV, Marapur SC, Kadam DV (2010) Ionotropic gelation and polyelectrolyte complexation: the novel techniques to design hydrogel particulate sustained, modulated drug delivery system: a review. Dig J Nanomater Biostructures 5:241–248
27. Vicini S, Mauri M, Wichert J, Castellano M (2017) Alginate gelling process: use of bivalent ions rich microspheres. Polym Eng Sci 1:1–6. https://doi.org/10.1002/pen
28. Patil P, Chavanke D, Wagh M (2012) A review on ionotropic gelation method: novel approach for controlled gastroretentive gelispheres. Int J Pharm Pharm Sci 4:27–32
29. Mørch ÄA, Donati I, Strand BL, Skja G (2006) Effect of Ca $^{2+}$, Ba $^{2+}$, and Sr $^{2+}$ on alginate microbeads. Society. 7:1471–1480
30. Yurdasiper A, Sevgi F (2010) An overview of modified release chitosan, alginate and eudragit RS microparticles. J Chem Pharm Res 3:704–721
31. Rao T, Bhadramma N, Immanuelu I, Radhika M, Syamala K (2014) Design and in-vitro evaluation of gliclazide alginate beads for controlled release. Res Rev J Pharm Nanotechnol 2:37–44
32. Aswathy KS, Abraham AM, Jomy L, John RK (2014) Formulation and evaluation of etodolac alginate beads prepared by ionotropic gelation for sustained release. J Sci Innov Res JSIR 3:527–531 http://www.jsirjournal.com/Vol3_Issue5_11.pdf
33. Sepúlveda-Rivas S, Fritz HF, Valenzuela C, Santiviago CA, Morales JO (2019) Development of novel EE/alginate polyelectrolyte complex nanoparticles for lysozyme delivery: physicochemical properties and in vitro safety. Pharmaceutics. 11:103. https://doi.org/10.3390/pharmaceutics11030103
34. Kotagale N, Raut N, Umekar M, Deshmukh P (2013) Zinc cross-linked hydroxamated alginates for pulsed drug release. Int J Pharm Investig 3:194. https://doi.org/10.4103/2230-973x.121292
35. Alkhayer G, Khudr H, Koudsi Y (2020) Enantioselective release behavior of ketoprofen enantiomers from alginate-metal. Anal Bioanal Chem Reserch 7:61–76. https://doi.org/10.22036/ABCR.2019.177147.1329
36. Üner M, Gönüllü Ü, Yener G, Altinkurt T (2005) A new approach for preparing a controlled release ketoprofen tablets by using beeswax. Farmaco. 60:27–31. https://doi.org/10.1016/j.farmac.2004.08.008
37. Bruschi ML (2015) Strategies to modify the drug release from pharmaceutical systems, Woodhead, 1st edn
38. Alkhayer G, Khudr H, Koudsi Y (2020) Spectroscopic and chromatographic investigation of chiral interactions between tiaprofenic acid and alginate-metal-complexes. RSC Adv 10:35121–35130. https://doi.org/10.1039/d0ra07665a
39. Paarakh MP, Jose P.ANI, Setty CM, Peter GV (2018) Release kinetics – concepts and applications, Int J Pharm Res Technol 8:12–20. https://doi.org/10.31838/ijprt/08.01.02.

40. Hasnain MS, Nayak AK (2019) Alginates: versatile polymers in biomedical applications and therapeutics,. Apple academic press; 1st ed, USA. https://doi.org/10.1017/CBO9781107415324.004
41. Idota Y, Kogure Y, Kato T, Yano K, Arakawa H, Miyajima C, Kasahara F, Ogihara T (2016) Relationship between physical parameters of various metal ions and binding affinity for alginate. Biol Pharm Bull 39:1893–1896. https://doi.org/10.1248/bpb.b16-00127
42. Tous S, Fathy M, Fetih G, Gad SF (2014) Preparation and evaluation of ketoprofen-loaded calcium alginate beads. Int J PharmTech Res 6:1100–1112

Publisher's Note